Detection of the Lunar Diurnal Atmospheric Tide

KEVIN HAMILTON

Department of Oceanography, University of British Columbia, Vancouver, B.C., Canada V6T 1W5

(Manuscript received 21 February 1984, in final form 30 April 1984)

ABSTRACT

A search was conducted for the principal lunar diurnal tide (O_1) in an 18½ year time series of twice-daily digitized sea level pressure analyses covering the region 20–90°N. At 20, 25, 30 and possibly at 35°N there is evidence for a systematic variation of the zonal wavenumber one harmonic of the pressure as a function of the phase of the O_1 tidal potential. This variation is clearly dominated by a westward traveling component (i.e., one that follows the tidal potential around the earth each day). The computed amplitudes are very small (less than 0.01 mb), and north of 35°N the random meteorological noise obscures the O_1 tidal oscillation to the point where it cannot be detected from analysis of the present data.

1. Introduction

It has been known for over a century that lunar tidal forces produce small, but clearly detectable, motions in the earth's atmosphere (e.g., Chapman and Lindzen, 1970). In the conventional approach to the study of this phenomenon, the time variation of the lunar gravitational potential is separated into various sinusoidally varying components (Doodson, 1922). The largest of these components forces the principal semidiurnal tide M_2; the M_2 variation in atmospheric surface pressure has been determined at a large number of individual stations throughout the world (Haurwitz and Cowley, 1970a). The elliptic semidiurnal tide N_2, is considerably smaller, but the amplitude and phase of the N_2 barometric oscillation have still been reliably determined at a few stations (Malin and Chapman, 1970; Palumbo, 1975). Of the remaining components in Doodson's analysis, the one that appears most likely to be detectable is the principal lunar diurnal tide O_1. Attempts have been made to determine the O_1 pressure oscillation from observations at several locations (Malin and Chapman, 1970; Palumbo, 1975). Only at Hong Kong and Naples have the computed amplitudes and phases been judged to be statistically significant. However, the phases determined at Hong Kong and Naples differ by almost 90°. This discrepancy led Matsuno (1980) to reexamine the Hong Kong data (along with data at other stations) in an effort to confirm the existence of the O_1 tide. He simply calculated a high resolution power spectrum from long records of hourly barometric observations. While he found clear evidence for peaks at the M_2 and N_2 frequencies, he could not discover any indication of a concentration of power at the O_1 frequency.

All previous studies of the tidal pressure variations have employed barometric observations taken at individual stations. Another potential resource for such investigations is the archive of digitized surface pressure analyses that are routinely produced at operational meteorological centers. Such analyses, however, have the limitation of being available only once or twice each day. This turns out to be a very severe drawback in the determination of the (approximately semidiurnal) M_2 and N_2 tides. However, as will be shown below, twice daily analyses may be sufficient for the detection of the (approximately diurnal) O_1 tidal variation. In fact, it will be demonstrated that by appropriately processing 18½ years of these analyses it is possible to clearly express the main features of the O_1 pressure oscillation, at least in subtropical latitudes. The data used for this study are described in Section 2. The analysis of these data is detailed in Section 3, and the results are discussed in Section 4. The conclusions are summarized in Section 5.

2. Data

The data employed were in the form of 5° × 5° latitude–longitude grids of analyzed sea level pressure for the period July 1962–December 1980. These analyses were obtained from the Data Support Section of the National Center for Atmospheric Research, where they were produced by interpolation of higher resolution U.S. Navy operational analysis grids (see Jenne, 1975, chapters 2 and 14). The area covered extends from 20°N to the North Pole and the analyses were produced for Greenwich mean noon (1200 GMT) and midnight (0000 GMT). There are sometimes several grids missing in a particular month (although this problem virtually ceased after 1966). These data are discussed further by Trenberth and Paolino (1980).

The analyses were naturally produced from station and ship observations that were reduced to mean sea level with corrections that would be independent of the tidal potential. Thus the tidal variations in the analyses should be equivalent to those that would be found in the observations from a worldwide network of barometers fixed to the land and ocean surfaces.

3. Analysis procedure

The O_1 component of the gravitational potential at the earth's surface can be written (e.g., Chapman and Lindzen, 1970) as

$$V = C \sin(2\lambda) \sin(\theta + \phi), \tag{1}$$

where C is a constant, λ the latitude, ϕ the longitude (east as positive) and θ a phase angle that depends on universal time and which advances roughly 335° each mean solar day. To be more precise, θ can be expressed as

$$t_u - \nu - s, \tag{2}$$

where t_u is Greenwich mean time expressed in degrees (one hour equals 15°), s an angle measuring the progress of the mean moon in its orbit and ν the angle between the meridional planes containing the mean moon and mean sun (positive when the moon is east of the sun). Each solar mean day the angles s and ν advance roughly 12.19 and 13.18° respectively. Chapman and Lindzen (1970) give more precise expressions for s and ν in terms of the mean solar time that has elapsed since Greenwich noon on 31 December 1899.

The expression (1) represents a westward propagating zonal wavenumber one forcing. In the absence of topography and land–sea contrasts the surface pressure response should also be a westward propagating zonal wavenumber one disturbance, i.e.,

$$\begin{aligned} P_{O_1} &= A \sin(\theta + \phi + \delta), \\ &= A \sin(\theta + \delta) \cos\phi + A \cos(\theta + \delta) \sin\phi, \end{aligned} \tag{3}$$

where the amplitude A and phase angle δ will be functions only of latitude. A possible strategy for detecting the O_1 tidal barometric oscillation could be based directly on (3). However, when only a limited number of observations are available each day it is generally preferable to base tidal determinations on a series of differences between the pressures recorded at successive observation times (e.g., Chapman and Lindzen, 1970). Thus, applying expression (3) to the difference in pressure over a 12 h interval, one finds

$$\begin{aligned} &\Delta P_{O_1}(t) \\ &\equiv P_{O_1}(t) - P_{O_1}(t - 12\text{ h}) \\ &= A\{\sin[\theta(t) + \delta] - \sin[\theta(t - 12\text{ h}) + \delta]\} \cos\phi \\ &\quad + A\{\cos[\theta(t) + \delta] - \cos[\theta(t - 12\text{ h}) + \delta]\} \sin\phi. \end{aligned} \tag{4}$$

Given that θ advances through ~334.37° in 24 mean solar hours,

$$\theta(t - 12\text{ h}) = \theta(t) - \beta,$$

where $\beta \approx 167.18°$. Hence, (4) becomes

$$\begin{aligned} \Delta P_{O_1} &= A[\sin(\theta + \delta) - \sin(\theta - \beta + \delta)] \cos\phi \\ &\quad + A[\cos(\theta + \delta) - \cos(\theta - \beta + \delta)] \sin\phi. \end{aligned} \tag{5}$$

It is easy to show that (5) is equivalent to

$$\begin{aligned} \Delta P_{O_1} &= A[\sin^2\beta + (1 - \cos\beta)^2]^{1/2}[\sin(\theta + \delta + \psi) \\ &\quad \times \cos\phi + \cos(\theta + \delta + \psi) \sin\phi], \end{aligned} \tag{6}$$

where

$$\psi = \arctan[\sin\beta/(1 - \cos\beta)],$$

or

$$\begin{aligned} \Delta P_{O_1} &= 1.987A \sin(\theta + \delta + 6.41°) \cos\phi \\ &\quad + 1.987A \cos(\theta + \delta + 6.41°) \sin\phi. \end{aligned} \tag{7}$$

This expression is the basis for the following procedure.

Whenever there were two surface pressure analyses available at a 12 h interval, a pressure tendency field was constructed by simply subtracting the analyzed values at each grid point, i.e.,

$$\Delta P_{obs}(t) = P_{obs}(t) - P_{obs}(t - 12\text{ h}). \tag{8}$$

Then for each available time and each 5° of latitude between 20 and 50°N, ΔP_{obs} was Fourier analyzed to determine the coefficients of the zonal wavenumber one harmonic, so that at a particular latitude

$$\Delta P_{obs}(t) \equiv \text{constant} + B_s(t) \sin\phi + B_c(t) \cos\phi + \cdots. \tag{9}$$

Each time t is associated with a particular lunar phase $\theta(t)$, and each of the determinations of B_s and B_c can be grouped into one of 12 classes depending on whether the θ value falls in the intervals 0–30°, 30–60°, ··· or 330–360°. After this analysis had been applied to the entire 18½ year period and to each latitude between 20 and 50°N, all the determinations of B_s and B_c for a particular phase class and latitude were averaged. This averaging should greatly reduce the random meteorological noise, but leaves intact any component of the pressure tendency that has a systematic dependence on the lunar phase. By plotting out the 12 average $B_s(B_c)$ determinations at θ values of 15, 45, ··· 345°, one obtains a rough graphical representation of the θ dependence of the $\sin\phi(\cos\phi)$ harmonic of the 12 h pressure tendency. The functions represented in such plots can be denoted by $\bar{B}_s(\theta)$ and $\bar{B}_c(\theta)$, so that the "observed" O_1 component of the pressure tendency is

$$\Delta P_{O_1} = \bar{B}_s(\theta) \sin\phi + \bar{B}_c(\theta) \cos\phi. \tag{10}$$

If a lunar diurnal pressure variation exists, then the behavior of $\bar{B}_s$ and $\bar{B}_c$ should be sinusoidal in θ. If

the pressure variation consists simply of a westward traveling wave then, comparing (10) with (7), one also expects that the amplitude of the $\bar{B}_s(\theta)$ and $\bar{B}_c(\theta)$ sinusoids should be identical and that the $\bar{B}_s$ curve should lead the $\bar{B}_c$ curve by 90°.

4. Results

A total of 12 818 12-hour pressure tendencies could be computed from the 18½ years of analyses. The numbers in each 30° lunar phase class were almost equal (ranging from 1061 to 1075). The dots in Fig. 1 display the results for $\bar{B}_s(\theta)$ for each of the 12 phase classes at four individual latitudes (20, 25, 30 and 35°N). These dots have been connected by line segments to provide a visual guide. Figure 2 gives the same results for $\bar{B}_c$.

Inspection of Figs. 1 and 2 reveals that at 20, 25 and 30°N there is a certain amount of systematic variation of $\bar{B}_s$ and $\bar{B}_c$ with the phase of the O_1 tidal potential. At 35°N the noise level rises significantly and it is much more difficult to discern any reasonable pattern in the dependence of $\bar{B}_s$ or $\bar{B}_c$ on θ. At 40, 45 and 50°N (not shown), the noise levels are still higher and no lunar diurnal variation is evident in the plots of $\bar{B}_s(\theta)$ or $\bar{B}_c(\theta)$.

At 20, 25 and 30°N it is not unreasonable to characterize the θ-dependence of $\bar{B}_s$ and $\bar{B}_c$ as being the sum of a sinusoid plus random noise. The smooth curves in Figs. 1 and 2 show the sinusoids determined from a least squares fit to the dots, i.e., at a particular latitude

$$\left.\begin{aligned}\bar{B}_s(\theta) &\approx D_s \cos(\theta + \gamma_s)\\ \bar{B}_c(\theta) &\approx D_c \sin(\theta + \gamma_c)\end{aligned}\right\}. \tag{11}$$

Table 1 gives the values of D_s, D_c, γ_s, γ_c at each latitude. From this point $\bar{B}_s$ and $\bar{B}_c$ will be assumed to have only sinusoidal dependence on θ, so that the "observed" O_1 pressure tendency can be written

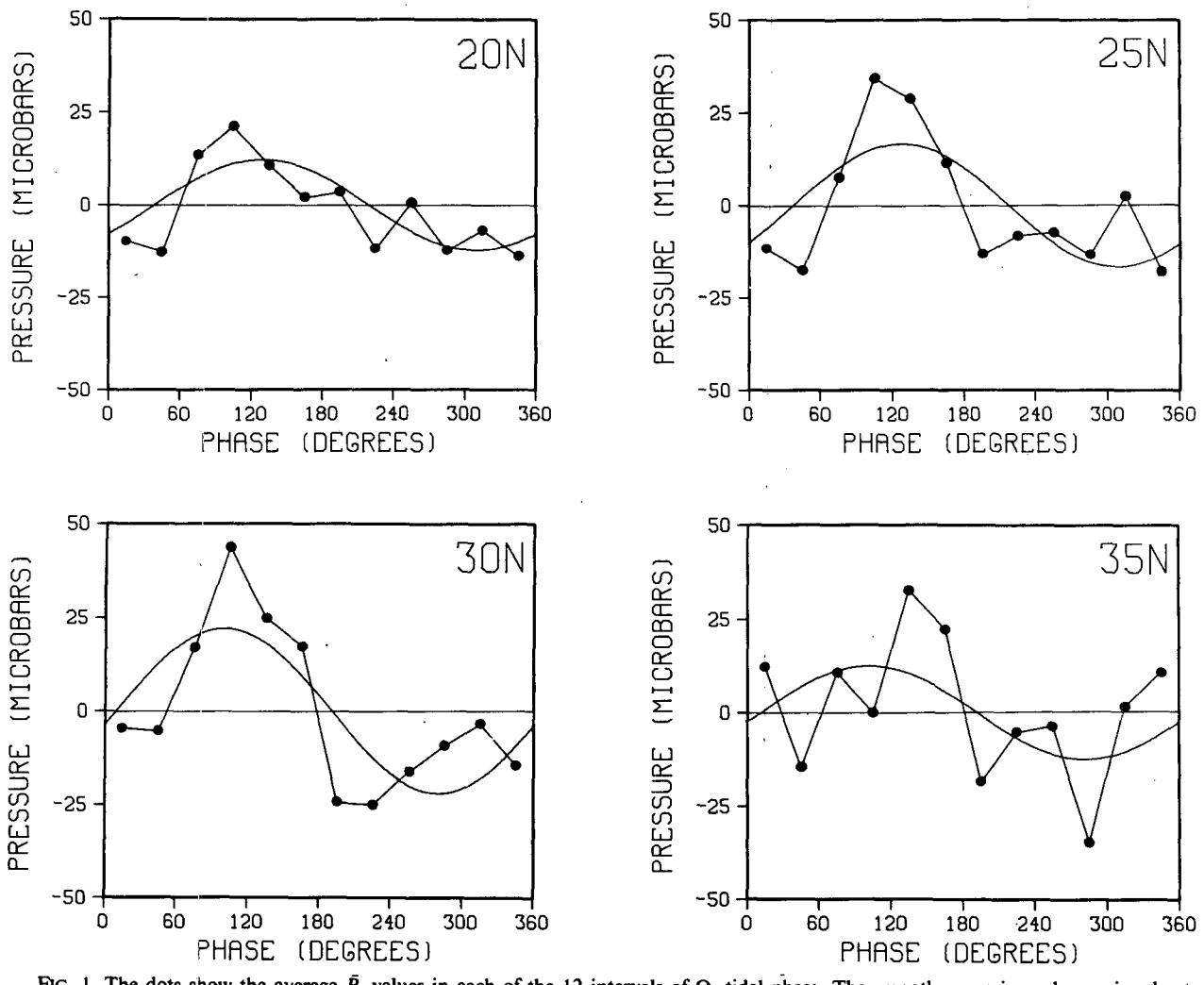

FIG. 1. The dots show the average $\bar{B}_s$ values in each of the 12 intervals of O_1 tidal phase. The smooth curve in each case is a least-squares fit of a sinusoidal to the dots. See text for details. For four latitudes: 20, 25, 30 and 35°N.

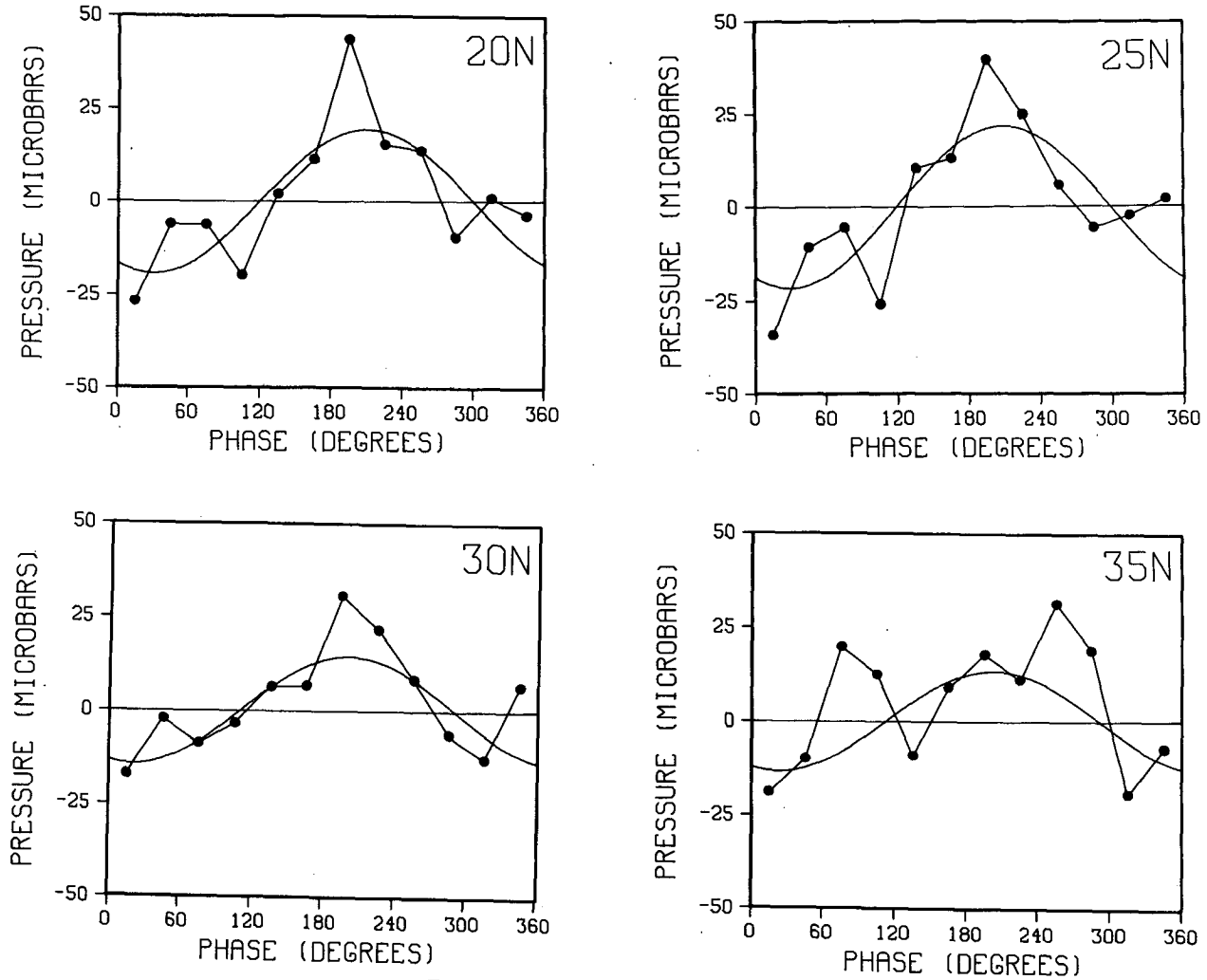

FIG. 2. As in Fig. 1 but for the $\bar{B}_c$ values.

$$\Delta P_{O_1} = D_s \cos(\theta + \gamma_s) \sin\phi + D_c \sin(\theta + \gamma_c) \cos\phi. \tag{12}$$

Expression (12) can be decomposed into eastward and westward propagating waves

$$\Delta P_{O_1} = \bar{D} \sin(\theta + \phi + \bar{\gamma}) + D^* \sin(-\theta + \phi - \gamma^*), \tag{13}$$

where it can be shown that for the westward propagating wave

$$4\bar{D}^2 = (D_s \cos\gamma_s + D_c \cos\gamma_c)^2 + (D_s \sin\gamma_s + D_c \sin\gamma_c)^2,$$

$$\tan\bar{\gamma} = (D_s \sin\gamma_s + D_c \sin\gamma_c)/(D_s \cos\gamma_s + D_c \cos\gamma_c),$$

while for the eastward propagating wave

$$4(D^*)^2 = (D_s \cos\gamma_s - D_c \cos\gamma_c)^2 + (D_s \sin\gamma_s - D_c \sin\gamma_c)^2,$$

$$\tan\gamma^* = (D_s \sin\gamma_s - D_c \sin\gamma_c)/(D_s \cos\gamma_s - D_c \cos\gamma_c).$$

TABLE 1. The parameters that characterize the observed sinusoidal O_1 time variation of the zonal wavenumber one harmonic of the pressure tendency (D_s, γ_s, D_c, γ_c, $\bar{D}$, $\bar{\gamma}$, D^*, γ^*) and the pressure itself (A, δ); see text for details. D_s, D_c, $\bar{D}$, D^* and A are all given in microbars.

Latitude	D_s	γ_s	D_c	γ_c	$\bar{D}$	$\bar{\gamma}$	D^*	γ^*	A	δ
20°N	12.2	−128.8°	19.3	−120.1°	15.7	−123.5°	3.7	74.2°	7.9	−129.9°
25°N	16.6	−127.1°	21.6	−119.2°	19.1	−122.6°	2.8	84.7°	9.6	−129.0°
30°N	21.9	−99.9°	14.5	−110.3°	18.1	−104.1°	4.1	−78.9°	9.1	−110.5°
35°N	12.5	−101.7°	13.5	−112.4°	12.9	−107.3°	1.3	5.3°	6.5	−113.7°

The values of $\bar{D}$, $\bar{\gamma}$, D^*, γ^* calculated from the D_c, γ_c, D_s, γ_s are listed in Table 1. At each latitude $\bar{D}$ is at least four times as large as D^*; therefore, the observed O_1 pressure variations are dominated by the westward traveling wave [i.e., the wave that follows the phase propagation of the potential, see Eq. (1)]. In addition, it is worth noting that the phases determined for the westward propagating wave appear to be reasonably coherent at the different latitudes, while this is certainly not true in the case of the eastward traveling wave.

Finally, the observational estimate for the amplitude A and phase δ of the westward traveling zonal wavenumber one O_1 pressure variation [see Eq. (3)] can be found simply by comparing (13) with (7), i.e.,

$$A = \bar{D}/1.987,$$
$$\delta = \bar{\gamma} - 6.41°. \quad (14)$$

The present estimates of A and δ are also given in Table 1.

It is of interest to compare the present results for the O_1 pressure oscillation with the well-known behavior of the M_2 barometric tide. The M_2 tidal potential at the earth's surface is of the form

$$V_{M_2} = F \cos^2\lambda \sin(2\eta + 2\phi), \quad (15)$$

(Chapman and Lindzen, 1970), where F is a constant and η is a phase angle that advances through 360° each lunar day ($\eta = t_u - \nu$). The observed M_2 barometric oscillation can be roughly approximated by

$$P_{M_2} \approx .055 \text{ mb } \cos^3\lambda \sin(2\eta + 2\phi - 15°), \quad (16)$$

(Chapman and Lindzen, 1970, pg. 94). The pressure response is very strongly dominated by a harmonic wave with the same zonal wavenumber and phase speed as the forcing potential itself (see Haurwitz and Cowley, 1970a, or Fig. 2L.4 of Chapman and Lindzen, 1970). This suggests that the effects of topography (and land–sea contrasts) on the M_2 tide are rather unimportant. There is no particular reason to suppose that topography should have any greater effect on the O_1 tide. Thus, it is extremely encouraging that the O_1 pressure variations found in the present study are dominated by a westward traveling component following the potential around the earth.

Expressions (15) and (16) show that the M_2 surface pressure response is roughly in phase with the tidal potential. On the other hand, the present results suggest that the O_1 barometric oscillation lags its forcing potential by ~110–130° (at least in the subtropics). There also appears to be a difference in the meridional variation of the amplitude between the M_2 and O_1 barometric oscillations; the amplitude of the M_2 tide decreases uniformly away from the equator, while there is a suggestion in Table 1 that the amplitude of the O_1 tide may have a local maximum near 25°N. It is, of course, the *gradient* of the potential that actually enters the governing tidal wave equations as a forcing term. Thus, given the radically different meridional structures of the M_2 and O_1 potentials [compare Eqs. (1) and (15)], it is not surprising that the tidal responses should be dissimilar. It is worth noting, however, that the amplitude of the M_2 and O_1 tides both drop off with increasing latitude faster than the forcing potential itself.

Theoretical predictions suggest that there should be a resonant atmospheric normal mode with a period a little (20%) larger than that of the O_1 tide [specifically the gravest antisymmetric zonal wavenumber one mode; (Longuet-Higgins, 1967)]. The meridional structure of this mode does bear some resemblance to the structure of the O_1 pressure response found in this study (see Fig. 10 of Longuett-Higgins, 1967). Thus, it might be possible to interpret the present findings in terms of a resonator being forced at a slightly higher frequency than that of its free oscillation (this might also explain the large phase difference between the forcing and the pressure response).

In Palumbo's (1975) analysis of the O_1 barometric oscillation at Naples (40.2°N) he found an amplitude of 0.0117 mb and a phase of −127°. This phase is consistent with the present determination, but Palumbo's amplitude would appear to be considerably larger than the present results at 35°N. However, it is noteworthy that Palumbo had to place rather large error bounds on his determination (0.0057 mb for the radius of the probable error circle). Malin and Chapman's (1970) results for Hong Kong (20.3°N) are more difficult to reconcile with the present observations. They determined a phase for the O_1 barometric oscillation of 158° (−202°) and an amplitude of 0.0167 mb (their radius of the probable error circle was 0.0033 mb). This phase differs by about 70° from the present determinations of δ at 20 and 25°N, and the Hong Kong amplitude is 80% larger than the present estimates of A at 20 and 25°N.

5. Conclusion

This paper has demonstrated the existence of an O_1 tidal variation in the atmosphere by means of a simple averaging of observed pressure tendencies according to lunar phase classes. The spirit of the analysis and presentation of the data is similar to that of Haurwitz and Cowley (1970b) who composited a large number of pressure differences between successive observation times (at a single station) to produce what they termed a "direct demonstration" of the existence of the M_2 tide. In the present study the use of grid-point analyses (rather than individual station pressures) has made possible the detection of the much smaller O_1 tide.

Despite the large number of data employed, the

O_1 barometric oscillation could be clearly seen at only 20, 25 and 30°N. In this latitude band the amplitude of the O_1 pressure variation can be estimated as ~0.008 mb and it appears that the maximum in surface pressure lags the maximum in the tidal potential by ~120°.

Acknowledgments. The author would like to thank Professor T. Matsuno for helpful comments. This work was supported by the Canadian Natural Sciences and Engineering Research Council through Grant UO219.

REFERENCES

Chapman, S., and R. S. Lindzen, 1970: *Atmospheric Tides.* Gordon and Breach, 200 pp.

Doodson, A. T., 1922: The harmonic development of the tide-generating potential. *Proc. Roy. Soc. London,* **A100,** 305–329.

Haurwitz, B., and A. D. Cowley, 1970a: The lunar barometric tide, its global distribution and annual variation. *Pure Appl. Geophys.,* **75,** 1–29.

——, and ——, 1970b: A direct demonstration of the lunar barometric tide. *Z. Geophys.,* **36,** 771–775.

Jenne, R. L., 1975: Data sets for meteorological research. NCAR Tech. Note TN/IA-111, 194 pp. [Available from the Publications Office, NCAR, P.O. Box 3000, Boulder, CO 80307.]

Longuet-Higgins, M. S., 1967: The eigenfunctions of Laplace's tidal equation over a sphere. *Phil. Trans. Roy. Soc.,* **A269,** 511–607.

Malin, S. R. C., and S. Chapman, 1970: Lunar tidal components O_1 and N_2 in the atmospheric pressure. *Pure Appl. Geophys.,* **80,** 309–318.

Matsuno, T., 1980: A trial search for minor components of lunar tides and short period free oscillations of the atmosphere in surface pressure data. *J. Meteor. Soc. Japan,* **58,** 281–285.

Palumbo, A., 1975: Lunar tides in meteorological data. *Quart. J. Roy. Meteor. Soc.,* **101,** 995–1001.

Trenberth, K. E., and D. A. Paolino, Jr., 1980: Northern Hemisphere sea-level pressure data set: Trends, errors and discontinuities. *Mon. Wea. Rev.,* **108,** 855–872.